

## **Appendix C**

### **Description of the Extended RADM Model**



## 1. Model Description

The Regional Acid Deposition Model (RADM) (Chang et al., 1987) was used as the basis for the Extended RADM. The RADM is an Eulerian model that was developed under the National Acidic Precipitation Assessment Program (NAPAP) to address regional photochemistry, aqueous chemistry, cloud processes, transport and wet and dry deposition. A primary deficiency in the use of RADM to study nitrogen deposition and inorganic particles, however, was the lack of representation of the important role of  $\text{NH}_3$  to affect deposition and particle composition through conversion of  $\text{HNO}_3$  to  $\text{NO}_3^-$  and of  $\text{NH}_3$  to aerosol  $\text{NH}_4^+$ . In order to synthesize the current knowledge of the processes governing the fate of inorganic nitrogen in a consistent modeling framework, RADM was enhanced, by adding several additional modules to represent the various atmospheric physical and chemical pathways governing the fate of emitted  $\text{NH}_3$ . These processes, their model representation, and assumptions in their formulation are described here.

The partitioning of reduced and oxidized nitrogen forms between the gas and the aerosol phases is governed by thermodynamic equilibrium (Seinfeld and Pandis, 1998). To model this partitioning, an additional process module representing aerosol equilibrium was added to the RADM framework. This module calculates equilibrium chemical composition of the sulfate-nitrate-ammonium-water aerosol, and is based on the work of Saxena et al. (1986) with further modifications described in Binkowski and Shankar (1995) and Binkowski (1999). Zhang et al. (2000) compared the performance of this thermodynamic module with other more comprehensive approaches and found results to be comparable for the sulfate-nitrate-ammonium-water system.

Two additional species, representing particulate  $\text{NH}_4^+$  and particulate  $\text{NO}_3^-$ , were also added to RADM. Existing transport modules were modified to account for advective and turbulent transport and dry deposition of these additional particulate species. The dry deposition velocities for particulate  $\text{NH}_4^+$  and  $\text{NO}_3^-$  were set to be the same as that of  $\text{SO}_4^{2-}$  already computed in RADM, and are based on the assumption of an internally mixed aerosol. Further, no distinction of aerosol size was retained since inorganic particles over the continental region are primarily in the fine aerosol size fraction. The representation of aqueous chemistry was modified to include the participation of particulate nitrate and ammonium. Further, the cloud transport and cloud scavenging portions of the model were modified to include the impact of these important processes in the representation of particulate ammonium and nitrate and to include their contribution to the eventual ammonium and nitrate wet deposition amounts. This enhanced version of the model is termed the *Extended-RADM*.

RADM was developed with grids that are 80-km on a side. More recently, a 20-km grid covering the northeastern U.S. nested within the 80-km grid was created for Chesapeake Bay studies as a one-way nest. For this study, the 20-km grid was extended south to include all of North and South Carolina. Both grids are shown in Figure C-1. The extended 20-km grid is the principal grid used for this assessment.

The RADM parameterization of dry deposition velocities for various gaseous species, including  $\text{NH}_3$ , is based on the resistance analog method of Wesley (1989) and is detailed in Chang et al. (1990) and Walmsley and Wesley (1996). The value of the deposition velocity,  $V_d$ , is dependent on three terms representing the bulk properties of the lower atmosphere and the underlying surface: the aerodynamic resistance ( $r_a$ ), the laminar sub-layer resistance ( $r_b$ ), and the canopy resistance ( $r_c$ ). For the various cases considered in this study, over most of the continental eastern U.S. we found the mean daytime values of  $V_d$  computed using this approach to be about 0.5-0.7  $\text{cm s}^{-1}$ . These estimates are considerably lower than those reported in the

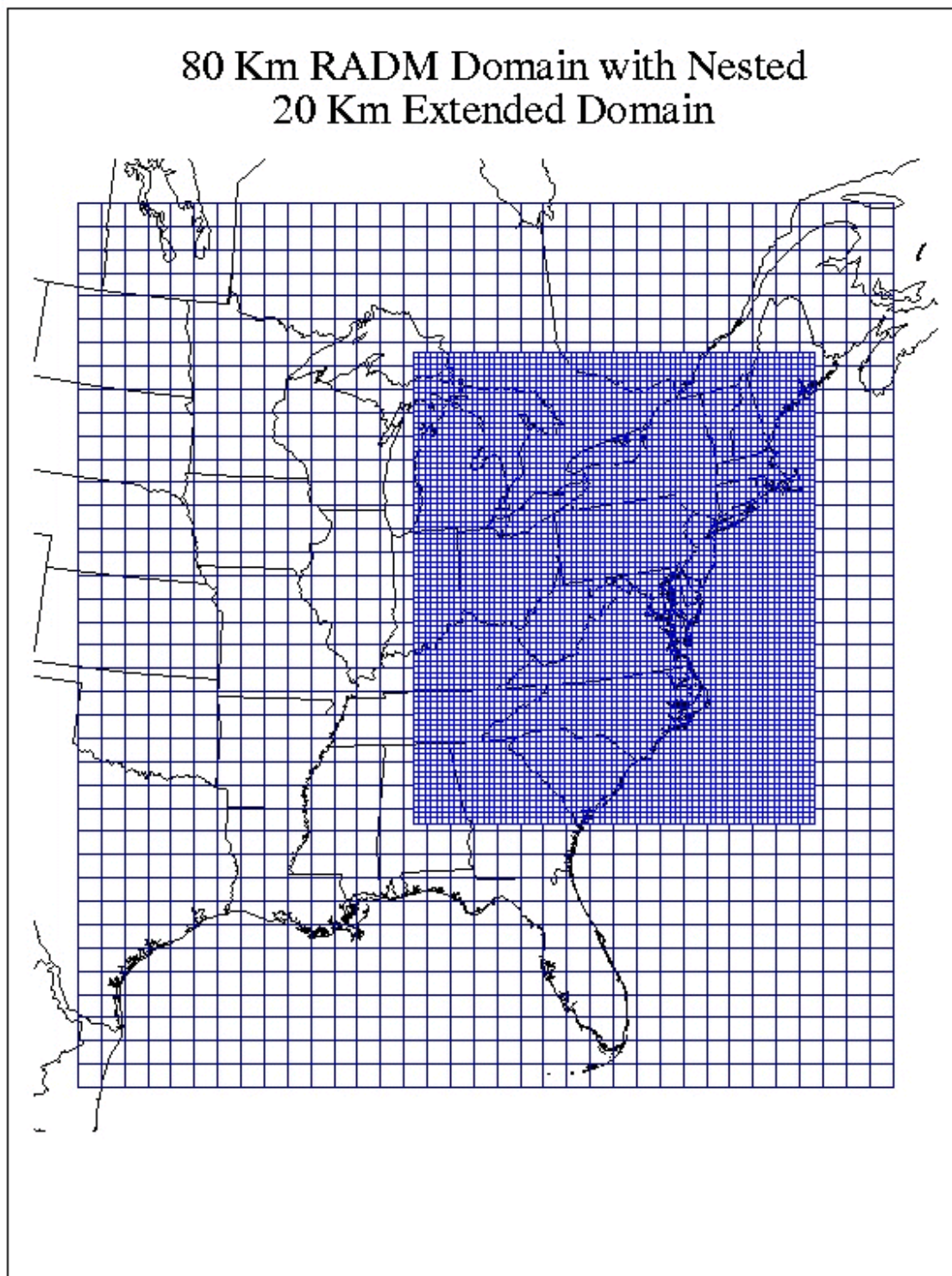


Figure C-1. Map of the 80-km grid Eastern U.S. domain with the embedded 20-km nest covering the mid-Atlantic and midwest regions.

measurements discussed earlier, but cannot be verified given the lack of comprehensive observational data on  $\text{NH}_3$  deposition velocity over the eastern U.S. These lower estimates of  $V_d$  could be related to the computed canopy resistance ( $r_c$ ) in the model. The  $r_a$  and  $r_b$  are dependent on prevalent meteorological conditions and standard methods for their estimation are widely used (Wesley and Hicks, 2000). The canopy or surface resistance describes the uptake process at the surface and in turn is dependent on the vegetative characteristics of the underlying surface, with smaller  $r_c$  for surfaces with stronger uptake. The  $r_c$  parameterization in RADM was inferred from limited deposition measurements for other species (e.g.,  $\text{SO}_2$ ) since reliable measurements of atmospheric  $\text{NH}_3$  were lacking. It appears that this approach results in modeled  $r_c$  values which are overestimated. To account for this overestimation and to be more consistent with European measurements, we modified the calculation of the  $\text{NH}_3$  deposition velocity through reducing the computed canopy resistance for  $\text{NH}_3$ , by one-third. (For a description of the European measurements see Mathur and Dennis, in press.) Though somewhat approximate, this simplistic approach yields  $V_d$  values in the upper range of 1-1.25  $\text{cm s}^{-1}$ , while retaining the regional spatial heterogeneity in its distribution due to variations in micrometeorology, land-use, and surface wetness (Walmsley and Wesley, 1996).

The thickness of the lowest model layer used in this study was 75 m. In Eulerian model calculations, inadequate resolution of the lowest model layer thickness can potentially create a bias in the estimated dry deposition. RADM uses a constant flux regime computation to deal with estimation of  $r_a$  and takes the surface layer thickness into account (Byun, 1990 and 1991). The turbulent flux is integrated over the lower height of the cell to compute  $r_a$ . During day time conditions, when the PBL height is high relative to the height of the lowest layer, the constant flux concept is valid (the eddy diffusivity,  $K_z$ , near the surface monotonically increases with height) and the bias in  $V_d$  is small and typically on the order of  $\pm 20\%$  (Byun and Dennis 1995). Under these conditions, ambient concentrations are relatively well mixed in the vertical; thus, the bias in deposition due to layer thickness is small. At night, under stable conditions, the constant flux concept may not be entirely valid, leading to  $r_a$  being a factor of 2-4 too high. However, RADM has been shown to systematically over-predict nighttime surface-level concentrations by factors of 2 and larger (Dennis, et al, 1990a). For nighttime calculations of deposition, these two biases are in opposite directions and to a large degree cancel each other out. Because the nighttime  $V_d$  is typically much smaller than the daytime  $V_d$ , the overall deposition bias is estimated to be the order of +20% to -50%. Given the large uncertainty in deposition velocity estimates, this degree of bias is considered acceptable.

Unlike most gas phase pollutants, which are consistently deposited,  $\text{NH}_3$  is both emitted from and deposited to land and water surfaces (Quinn et al., 1988; Asman et al., 1994). In characterizing the air-surface exchange of  $\text{NH}_3$ , several measurement studies point towards the existence of a "compensation point" (e.g., Farquhar et al., 1979; Lemon and Van Houtte, 1980). These studies report that, depending on whether the difference between  $\text{NH}_3$  concentrations in the air and those in the depositing surface is positive or negative, either dry deposition to the surface or emission from the surface could occur. This could imply that there may be no  $\text{NH}_3$  dry deposition to surfaces that contain substantial amounts of  $\text{NH}_3$ , such as fields within a few weeks of spreading of manure or cattle-grazing meadows (Asman and van Jaarsveld, 1992). Asman and Janssen (1987) estimated average annual reductions in  $\text{NH}_3$  deposition on the order of 20% for such fields. Measurements from Langford and Fehsenfeld (1992) demonstrated that under circumstances of high atmospheric  $\text{NH}_3$  concentrations, a pine forest acted as a sink, but it acted as a source at low  $\text{NH}_3$  concentrations. These studies imply that natural vegetation may be a net sink in the vicinity of source regions but a net source of  $\text{NH}_3$  in regions where un-neutralized

acidic aerosols could depress gaseous  $\text{NH}_3$  concentrations below the compensation point. The representation of this bi-directional air-surface exchange in regional models employing relatively coarse grid resolution is challenging, however, because detailed information on land management practices employed for the mosaic of land-use categories represented within each coarse model grid cell is currently lacking. Further, the characterization of this net  $\text{NH}_3$  emission from surfaces such as intensively grazed pastures and fertilized croplands requires detailed information on local surface environmental conditions, including form of nitrogen input,  $\text{NH}_x$  status in plant leaves, nitrogen status in the soil, plant growth stage, and micrometeorology. These conditions vary considerably spatially and temporally, are not typically well known, are subject to significant uncertainty, and are not likely to be resolved by model grid resolution typical of regional scale models. In addition, our intent in this study is to characterize mean seasonal and annual features of the distribution of  $\text{NH}_x$  compounds. We therefore ignore the explicit treatment of such  $\text{NH}_3$  emission sources, except where they are already accounted for in the base inventory (e.g., fertilized croplands).

## **2. Development of Annual Averages**

The Extended RADM is very computationally intensive because it predicts hourly photochemistry. Although recent advances in computational technology and computer code optimization have enabled the application of regional models over monthly to seasonal scales, their applications to study long-term pollutant behavior and deposition patterns over several seasonal and annual cycles challenge the practical limits of current computer resources. Aggregation techniques are available that combine into seasonal and annual totals a limited number of episodic estimates representing a variety of meteorological cases. Such approaches have emerged as useful practical methods for modeling the long-term relationships among changing emission patterns and regional air quality and atmospheric deposition. These techniques are based on the assumption that the atmospheric chemistry, transport, and deposition at a given location are governed by a number of different recurring weather patterns that can be combined to produce a realistic estimate of annual and seasonal synoptic and chemical climatology (Brook et al., 1995a).

The aggregation technique used here has been previously used during the NAPAP study to develop climatological seasonal and annual estimates of acid deposition totals (Dennis et al., 1990b). The approach involves the selection of a set of events for model simulations that are representative of the cross section of synoptic conditions occurring on a climatological annual cycle. Meteorological cases of 5-day durations during the 1979-1983 period were grouped by wind flow patterns through cluster analysis and sampled proportionate to their frequency of occurrence as detailed in Brook et al. (1995a, b). A total of 30 cases constitute the aggregation sample. The precipitation predicted for each case within a cluster was adjusted to the long-term mean precipitation for that cluster to estimate average deposition. This procedure was selected because the spatial pattern of precipitation during an individual event will not necessarily resemble the cluster average. The aggregation method produces a climatological average of transport and deposition representative of the transport of the 1980s and the seven-year average precipitation of that period. This precipitation average approximates well the 30-year normal precipitation.

### 3. Defining an Applications Version of the Extended RADM

To account for the low bias in the  $\text{NH}_3$  emission estimates for the U.S. from the 1985 NAPAP inventory, we developed seasonal correction factors for  $\text{NH}_3$  emissions through successive applications of the Extended-RADM and systematic comparisons with observed data. This simple “brute-force” inversion analysis allowed us to develop a seasonal modeling inventory for  $\text{NH}_3$  that, as will be discussed subsequently, provides model results that are consistent with observed values for both ambient atmospheric concentrations and wet deposition amounts. We adjusted the  $\text{NH}_3$  emission fields input to the Extended-RADM through successive model application and comparison with a suite of ambient and wet measurements. In these analyses, we included comparisons of model results against measurements of ambient levels of  $\text{HNO}_3$ ,  $\text{SO}_4^{2-}$ ,  $\text{NO}_3^-$ , and  $\text{NH}_4^+$  and wet deposition amounts of  $\text{SO}_4^{2-}$ ,  $\text{NO}_3^-$ , and  $\text{NH}_4^+$ , but gave more weight towards satisfying three specific criteria: 1) the adjustment in  $\text{NH}_3$  emissions should not disturb the modeled ambient and wet deposition for sulfate through perturbations in cloud pH-related oxidation pathways, such as through ozone oxidation, 2) since  $\text{NH}_3$  provides a pathway for formation of particulate  $\text{NO}_3^-$ , the predicted ambient  $\text{NO}_3^-/(\text{HNO}_3 + \text{NO}_3^-)$  ratio should retain the spatial regional signature indicated by measurements, and 3) any bias structure in modeled  $\text{NH}_4^+$  wet deposition should be similar to that for  $\text{SO}_4^{2-}$  and  $\text{NO}_3^-$  wet deposition. This approach provided a physically-based, self-consistent constraint for potential growth in  $\text{NH}_3$  emissions as opposed to a purely empirically based one in which  $\text{NH}_3$  increases are dictated solely by discrepancies between model and observed ambient  $\text{NH}_x$  levels without accounting for other modeled species.

Table C-1 presents the resulting estimated domain mean seasonal adjustment factors for  $\text{NH}_3$  emissions in the NAPAP inventory. The estimates are representative of the late 1980's to early 1990's period of ammonia emissions. These results suggest that on an annual basis, the 1985 NAPAP  $\text{NH}_3$  emissions inventory was a factor of 2.75 too low, confirming suspicions of previous studies (e.g., Chang et al., 1990) and giving annual emissions rates consistent with

EPA's 1990 National Emissions Inventory. Additionally, the adjustment factors showed a pronounced seasonal variation and yielded maximum  $\text{NH}_3$  emissions during summer, followed by spring, fall and winter. These trends are in agreement with recent  $\text{NH}_3$  flux measurements reported by Aneja et al. (2000), who observed similar seasonal variation in  $\text{NH}_3$  emissions from waste storage and treatment lagoons. It should be noted, however, that since the ambient and wet deposition measurements used in our simple inversion analysis were for the late 1980s to early 1990s period, the magnitude of regional estimated  $\text{NH}_3$  emissions should be taken as representative emissions only for that period. Also, since the method only scaled the emissions based on a fixed inventory, growth in local  $\text{NH}_3$  emissions was only captured to the extent that they were detailed in the base inventory. The seasonally-adjusted  $\text{NH}_3$  emissions were used in the model simulations. For this study, the  $\text{NH}_3$  emissions were kept constant at the effective 1990 levels.

Table C-1. Seasonal correction factors to the 1985 NAPAP ammonia emissions inventory developed for the Extended RADM

Season	Factor
Summer	4.9
Fall	1.32
Winter	1.31

#### **4. Comparison of Model Predictions with Measurements**

The development, application and evaluation of RADM, which formed the basis for the Extended RADM, has been documented extensively by NAPAP (Chang, et al. 1987, Chang, et al., 1990 and Dennis, et al., 1990a). RADM continued to undergo periodic peer review, evaluations and improvements since completion of the NAPAP assessment in 1991 (Dennis, et al., 1993; McHenry and Dennis, 1994; Cohen and Dennis, 1994; External Review Panel, 1994; Eder and LeDuc, 1996; Eder, et al., 1996). RADM has been used in more recent U.S. EPA studies of acidic deposition (e.g. U.S. EPA 1995), assessments of fine particle mass and light extinction, and assessments of deposition of nitrogen to coastal estuaries (Dennis 1997, U.S. EPA 1997). Here are presented comparisons specifically for the Extended RADM.

##### *a. Annual deposition and ambient concentrations*

To assess the performance of the Extended-RADM, annual predictions of both ambient concentrations and wet deposition amounts were compared with measurements from the Clean Air Status and Trends Network (CASTNet; CASTNet 2002) and precipitation chemistry data from the NADP (2002), respectively. To develop climatologically-representative measurements to compare with aggregated model results, we used several years of measurements from the CASTNet (1988-1992) and NADP (1984-1993) networks. Recognizing the intrinsic bias in using a small sample of precipitation events to approximate average rainfall (since no single storm event can replicate long-term average rainfall patterns), the modeled wet deposition amounts were scaled by climatologically observed precipitation within each model grid cell following the approach of Dennis et al. (1990b); these were then compared with measured wet deposition amounts. For the comparisons reported here, measurements from 44 CASTNet sites and 124 NADP sites located within the model domain were used. A 75% completeness criterion was used for averaging the ambient measurements from CASTNet. To minimize possible bias arising from missing data, a more stringent 90% completeness criterion was used in accumulating the NADP deposition measurements. Both networks have excellent spatial coverage across the eastern U.S. as shown in Figure C-2 and thus the comparisons provide an opportunity to assess the performance of the model in capturing the spatial variability in both ambient levels and wet deposition amounts.

The degree of correspondence between the modeled and measured ambient concentrations and wet deposition amounts was examined for various species both on a climatological annual and seasonal basis. In the subsequent discussion, we use the term correlation to denote this degree of correspondence between the model and measurements. Figure C-3 presents scatter-plots of the relationship between model predicted climatological annual averages and corresponding measurements of ambient concentrations and wet deposition amounts for selected ions that are important in determining aerosol composition and wet deposition amounts in the eastern United States. A summary of the comparisons in Figure C-3, plus additional comparisons between model- predicted, climatological annual averages and NADP and CASTNet measurements, is given in Table C- 2.



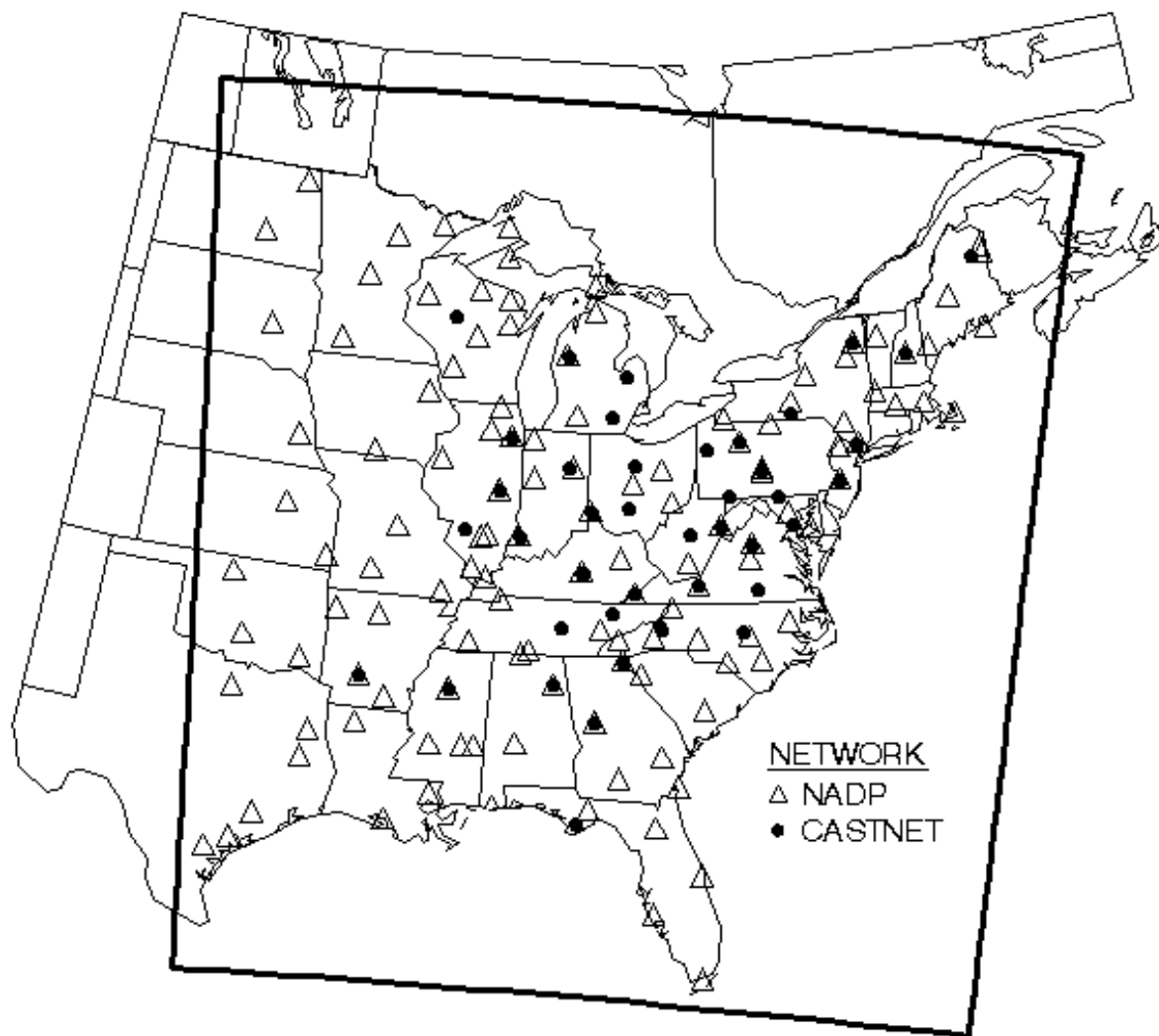


Figure C-2. Map of the Extended RADM Domain showing locations of the two monitoring networks, NADP and CASTNet, and their spatial coverage.

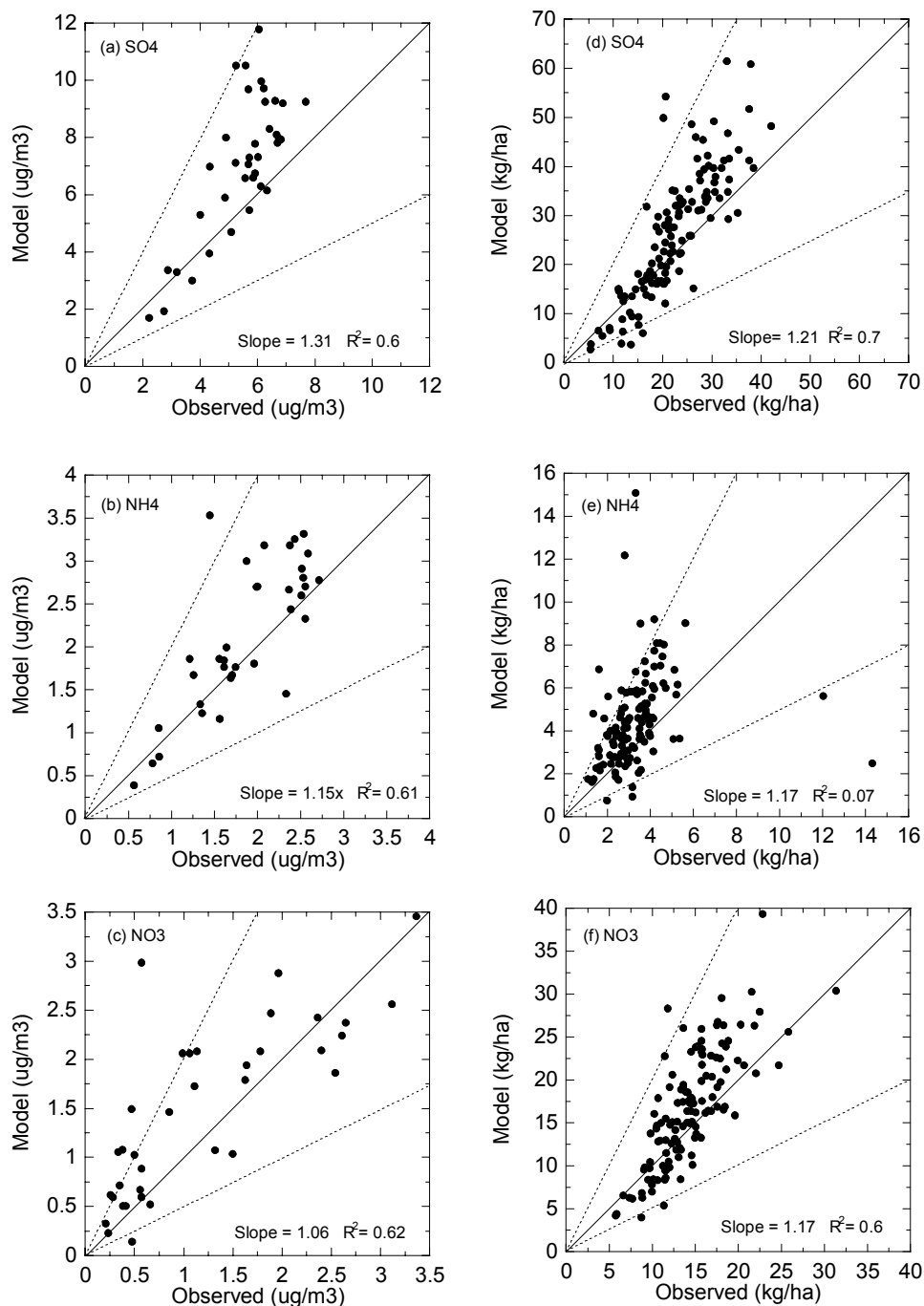


Figure C-3. Comparison of model simulated annual climatological averages with measurements: panels a to c are comparisons of ambient levels with CASTNet data; panels d to f are comparisons of wet deposition amounts with NADP data. The solid line indicates the 1:1 relationship, dotted lines indicate 1:2 and 2:1 comparison bounds as aids for judgment. Slope and coefficient of determination ( $r^2$ ) of the correlation between model and observed are indicated in each panel.

Table C-2. Summary of comparisons between predicted and measured values of wet and dry deposition.		
NADP Wet Deposition		
$\text{SO}_4^{=}$	Ext.RADM = 1.21 x NADP	$r^2 = 0.73$ , (n=124)
$\text{NH}_4^+$	Ext.RADM = 1.17 x NADP	$r^2 = 0.36$ , (n=121)*
$\text{NO}_3^-$	Ext.RADM = 1.17 x NADP	$r^2 = 0.64$ , (n=124)
CASTNet Ambient Concentrations		
$\text{HNO}_3$	Ext.RADM = 1.37 x CASTNet	$r^2 = 0.36$ , (n=44)
$\text{HNO}_3 + \text{NO}_3^-$	Ext RADM = 1.41 x CASTNet	$r^2 = 0.61$ , (n=44)
$\text{NO}_3^-$	Ext.RADM = 1.28 x CASTNet	$r^2 = 0.63$ , (n=44)
$\text{NO}_3^- / (\text{HNO}_3 + \text{NO}_3^-)$	Ext.RADM = 1.04 x CASTNet	$r^2 = 0.47$ , (n=43)
$\text{NH}_4^+$	Ext.RADM = 1.25 x CASTNet	$r^2 = 0.60$ , (n=41)

\* with the four outliers removed

In general, with the exception of  $\text{NH}_4^+$  wet deposition, good agreement for model predicted annual estimates are noted, with  $r^2$  in the range of 0.6-0.7 for both ambient concentrations (Figure C-3a-c) and wet deposition amounts (Figure C-3d-f). These correlations are reasonable, given that they are based on comparing grid-averaged values with point measurements (Schere, 1988; McKeen et al., 1991). It is difficult for a grid model operating from first principle descriptions of the processes, combined with comparing its grid predictions with point measurements, to achieve correlations greater than 0.7 ( $r^2 = 0.49$ ). The poor  $r^2$  for wet  $\text{NH}_4^+$  deposition (Figure C-3e) results from discrepancies between model and measurements at a few sites characterized by relatively large model over- and under-predictions, though the overall correlation was good (without the four outliers, the  $r^2 = 0.36$ ). Since similar outliers were not noted for  $\text{SO}_4^{2-}$  and  $\text{NO}_3^-$  wet deposition, these discrepancies in  $\text{NH}_4^+$  wet deposition can be attributed primarily to large uncertainties associated with spatial variability of  $\text{NH}_3$  emissions in the inventory. As discussed earlier, the  $\text{NH}_3$  emissions correction factors are intended to be regionally representative and do not account for local spatial variability in the emissions. Thus, if a particular source category is missing in the base inventory, the corrected emissions would still be under-estimated. Consequently, poor estimation of local  $\text{NH}_3$  emissions can contribute to local poor prediction of wet  $\text{NH}_4^+$  deposition. More recent modeling studies of  $\text{NH}_3$  indicate that large uncertainty in  $\text{NH}_3$  emissions can significantly affect model performance, supporting this conclusion (Gilliland 2001). For  $\text{HNO}_3$  during the warm half of the year when the spatial signal is more pronounced due to more active photochemistry, the  $r^2$  is 0.52, more comparable to wet nitrate deposition. For ambient  $\text{NO}_3^-$  during the cold half of the year when its spatial signal is more pronounced, the  $r^2$  is 0.71. The  $r^2$  of 0.61 for total nitrate ( $\text{HNO}_3 + \text{NO}_3^-$ ), for which there is less concern about measurement bias, is reasonable and the partitioning of total nitrate is basically unbiased, with an acceptable  $r^2$  of 0.47. Thus, we believe the Extended RADM to a

sufficient degree is capturing the spatial patterns in annual wet deposition, ambient concentrations and partitioning of key species.

*b. Growing season ozone*

The ozone predictions of relevance for ozone exposure analysis relate to the distribution of ozone during the growing season, rather than a seasonal average, because it is largely an hourly exposure above a defined threshold (e.g., 60 ppb) that is of concern. The ozone analysis for this assessment focused on daylight hours, for which the model does best and when ozone levels dominate the overall exposure. The model has a large nighttime bias (Byun and Dennis, 1995; Dennis et al., 1990a), but this is less relevant to estimation of the effects of ozone exposure because the plant stomata are more frequently closed at night. Daytime ozone predictions provide the most reliable indicators of change in ozone exposure. A concentration distribution of hourly ozone can be constructed for the Extended RADM to represent exposure during the growing season, using a warm-season subset of the aggregation cases. The daytime (8 a.m. to 8 p.m.) hourly ozone distribution from the Extended RADM, defined by the decile cutpoints, is compared to the daytime hourly and daytime maximum ozone distribution observed at SHEN across several years (1989-1995) in Figure C-4. The model distribution is in excellent agreement with the shape of the observed distribution, and is biased high by only about 10%. The model distribution is more similar to the high ozone years observed at SHEN and is between the maximum year distribution and the daily maximum distribution. These distributions are all quite similar because the diurnal ozone pattern is broad with little amplitude. Most of the range in the distribution comes from synoptic differences among days. The extent of agreement is unusually good.

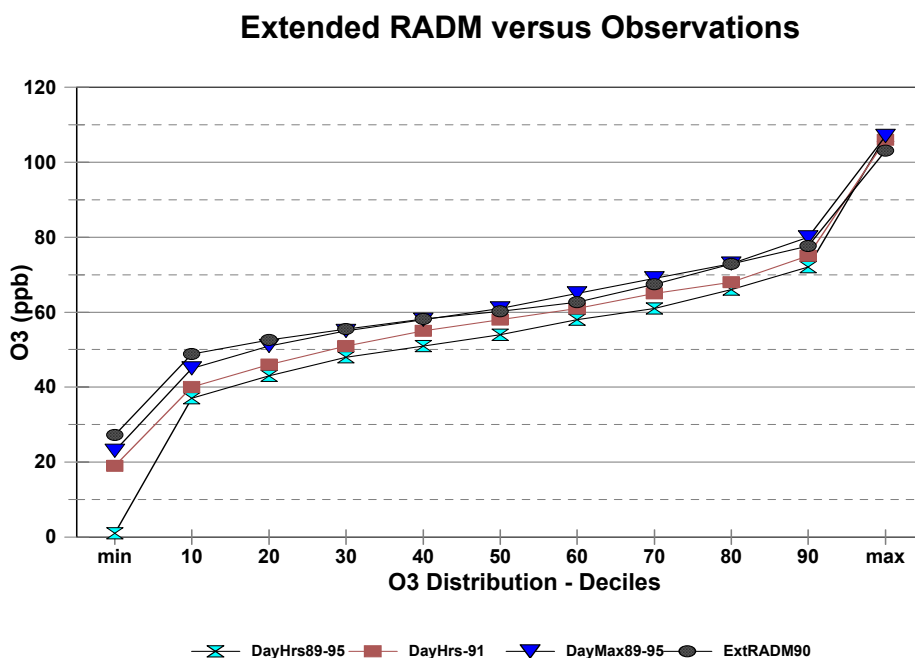


Figure C-4. Comparison of the growing season daytime (8 a.m. - 8 p.m.) ozone distribution predicted by the Extended RADM with the average distribution observed in SHEN from 1989 to 1995, the distribution for 1991, and the 1989 to 1995 daily maximum ozone distribution.

Given this degree of agreement, the Extended RADM should provide a reasonable vehicle for estimating changes in ozone exposure above a defined threshold for the growing season. It is key that the model does an adequate job of estimating the change in the upper end of the distribution. We should take into consideration, however, the observed 10% bias in the modeled ozone distribution. Also, we should consider that the system is potentially nonlinear in its response at different points along the distribution, in part because the number of hours per day above the defined threshold is not constant, but is itself a distribution. A representative threshold for the exposure change calculations from the model would not necessarily simply be the same threshold as defined for the ecological models. As demonstrated in the assessment calculations, the change in overall exposure-hours is dominated by the change in number of hours, rather than the change in the daily maximum ozone. Therefore, a threshold should be defined that best represents the overall pattern of hours above threshold. This was done for the Extended RADM. Several modeled hours-above-threshold distributions, using several model thresholds, were compared with the observed distribution above 60 ppb. The model hours-above-threshold distribution that was found to have a good match with the observed distribution of hours above 60 ppb, be consistent with the 10% bias, and show stable response across the emissions changes was a model threshold of 65ppb. The modeled (threshold = 65ppb) and observed (threshold = 60ppb) distributions are shown in Figure C-5. Thus, 65 ppb ozone was the threshold used with the Extended RADM in this assessment to best represent change in exposure associated with a “real world” threshold of 60ppb used by the ecological models. If the ecological model exposure threshold were to be changed, this procedure with the Extended RADM should be repeated to develop a new representative threshold. We believe the comparisons are sufficiently in agreement that this approach with the Extended RADM is reasonable and appropriate for the growing season exposure-hour calculations.

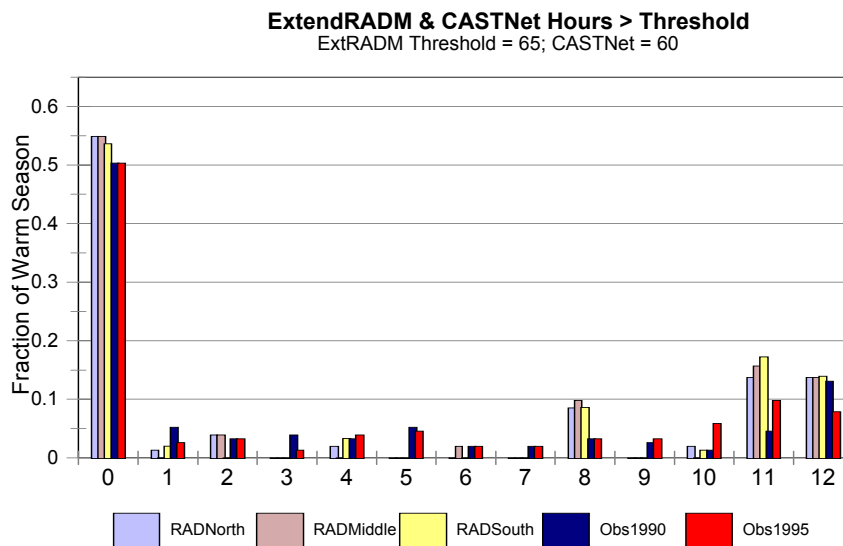


Figure C-5. Histogram of the number of growing-season daylight hours (8 a.m.-8 p.m.) within a day for which the defined threshold is exceeded for SHEN. Extended RADM  $O_3$  threshold = 65 ppb, measurements  $O_3$  threshold = 60 ppb. Extended RADM calculations are shown for the three cells covering the northern, middle and southern portions of SHEN.

## 5. References

- Aneja, V. P., J. P. Chauhan, and J. T. Walker, Characterization of atmospheric ammonia emissions from swine waste storage and treatment lagoons, *J. Geophys. Res.*, 105, 11,535-11,545, 2000.
- Asman, W. A. H. and A. J. Janssen, A long-range transport model for ammonia and ammonium for Europe, *Atmos. Environ.*, 21, 2099-2119, 1987.
- Asman, W. A. H. and H. A. van Jaarsveld, A variable resolution model applied for NH<sub>x</sub> in Europe, *Atmos. Environ.*, 26, 445-464, 1992.
- Asman, W. A. H., R. M. Harrison, and C. J. Ottley, Estimation of the net air-sea flux of ammonia over the southern bight of the north sea, *Atmos. Environ.*, 28, 3647-3654, 1994.
- Binkowski, F. S., and U. Shankar, The Regional Particulate Matter Model 1. Model description and preliminary results, *J. Geophys. Res.*, 100, 26,191-26,209, 1995.
- Binkowski, F. S., *Aerosols in Models-3 CMAQ, Chapter 10, Science Algorithms of the EPA Models-3 Community Multiscale Air Quality (CMAQ) Modeling System*, D. Byun and J. Ching (Eds.), EPA/600/R-99/030, Office of Research and Development, U.S. Environmental Protection Agency, 1999.
- Brook, J. R. P. J. Samson, and S. Sillman, Aggregation of selected three-day periods to estimate annual and seasonal wet deposition totals for sulfate, nitrate, and acidity. Part I: A synoptic and chemical climatology for eastern North America, *J. Applied Meteor.*, 34, 297-325, 1995a.
- Brook, J. R. P. J. Samson, and S. Sillman, Aggregation of selected three-day periods to estimate annual and seasonal wet deposition totals for sulfate, nitrate, and acidity. Part II: Selection of events, deposition totals, and source-receptor relationships, *J. Applied Meteor.*, 34, 326-339, 1995b.
- Byun, D.W., On the analytical solutions of flux-profile relationships for the atmospheric surface layer, *J. Applied Meteor.*, 29, 652-657, 1990.
- Byun, D.W., Determination of similarity functions of resistance laws for the planetary boundary layer using surface-layer-similarity functions, *Boundary Layer Meteorology*, 57, 17-48, 1991.
- Byun, D.W. and R.L. Dennis, Design artifacts in Eulerian air quality models: Evaluation of the effects of layer thickness and vertical profile correction on surface ozone concentrations, *Atmos. Environ.*, 29, 105-126, 1995.
- Clean Air Status Trends Network (CASTNet), World wide web site, <http://www.epa.gov/castnet>, 2002.
- Chang, J. S., R. A. Brost, I. S. A. Isaksen, S. Madronich, P. Middleton, W. R. Stockwell, and C. J. Walcek, A three-dimensional Eulerian acid deposition model: Physical concepts and formulation, *J. Geophys. Res.*, 92, 14,681-14,700, 1987.
- Chang, J. S., F. S. Binkowski, N. L. Seaman, D. W. Byun, J. N. McHenry, P. J. Samson, W. R. Stockwell, C. J. Walcek, S. Madronich, P. B. Middleton, J. E. Pleim, and H. L. Landsford, The regional acid deposition model and engineering model, *NAPAP SOS/T Report 4, in National Acid Precipitation Assessment Program, Acidic Deposition: State of Science and Technology, Volume I*, National Acid Precipitation Assessment Program, Washington, DC, 1990.

Cohn, R. D. and Dennis R. L., 1994. The Evaluation of Acid Deposition Models Using Principal Component Spaces, *Atmospheric Environment*, **28**, 2531-2543.

Dennis, R.L., F.S. Binkowski, T.L. Clark, S.J. Reynolds and S.K. Seilkop, Evaluation of regional acidic deposition models (Part I), *NAPAP SOS/T Report 5, in National Acid Precipitation Assessment Program: State of Science/Technology, Volume 1*, National Acid Precipitation Program, 722 Jackson Place, Washington D.C., 1990a.

Dennis, R.L., F.S. Binkowski, T.L. Clark, J.N. McHenry, S.J. Reynolds, and S.K. Seilkop, Selected applications of the regional acid deposition model and engineering Model, *Appendix 5F (Part 2) of NAPAP SOS/T Report 5, in National Acid Precipitation Assessment Program: State of Science and Technology, Volume I*, National Acid Precipitation Assessment Program, Washington, D.C., 1990b.

Dennis, R.L., J.N. McHenry, W.R. Barchet, F.S. Binkowski, and D.W. Byun, 1993. Correcting RADM's sulfate underprediction: Discovery and correction of model errors and testing the correction s through comparisons against field data. *Atmospheric Environment*, **27A**(6), 975-997.

Dennis R.L., 1997. Using the Regional Acid Deposition Model to Determine the Nitrogen Deposition Airshed of the Chesapeake Bay Watershed. in Joel E. Baker, editor, *Atmospheric Deposition to the Great Lakes and Coastal Waters*, Society of Environmental Toxicology and Chemistry, Pensacola, FL, pp 393-413.

External Review Panel. 1994: Report on RADM evaluation for the Eulerian Model Evaluation Field Study Program, Anton Eliassen, editor. Norwegian Meteorological Institute, Norway.

Eder B.K. and S.K. LeDuc, 1996. Can selected RADM simulations be aggregated to estimate annual concentrations of fine particulate matter? In *Measurement of toxic and related air pollutants*. VIP-64. Proceedings of an International Specialty Conference, Research Triangle Park, NC, May 7-9, 1996. Air & Waste Management Association, Pittsburgh, PA, pp 732-739.

Eder B.K., S.K. LeDuc, and F.D. Vestal, 1996. Aggregation of selected RADM simulations to estimate annual ambient air concentrations of fine particulate matter. in Preprints, Ninth Joint conference of Applications of Air Pollution Meteorology with A&WMA, January 28-February 2, 1996, Atlanta, Georgia. American Meteorological Society, Boston, MA, pp 390-392.

Farquhar, G.D., R. Wetselaar, and P.M. Firth, Ammonia volatilization from senescing leaves of maize, *Science*, **203**, 1257-1258, 1979.

Gilliland, A.B., R.L. Dennis, S.J. Roselle, T.E. Pierce, and L.E. Bender, Developing seasonal ammonia emission estimates with an inverse modeling technique, *Proc. of the 2<sup>nd</sup> International Nitrogen Conference on Science and Policy, TheScientificWorld*, 1(S2), 356-362, 2001.

Langford, A.O. and F.C. Fehsenfeld, Natural vegetation as a source or sink for atmospheric ammonia: A case study, *Science*, **255**, 581-583, 1992.

Lemon, E. and R. Van Houte, Ammonia exchange at the land surface, *Agron. J.*, **72**, 876-883, 1980.

Mathur R. and R. L. Dennis, 2003. Seasonal and Annual Modeling of Reduced Nitrogen Compounds Over the Eastern United States: Emissions, Ambient Levels, and Deposition Amounts, *Journal of Geophysical Research*, (in press).

- McHenry, J. N. and R. L. Dennis, The relative importance of oxidation pathways and clouds to atmospheric ambient sulfate production as predicted by the regional acid deposition model, *J. Appl. Meteor.*, 33, 890-905, 1994.
- McKeen, S.A., E.-Y. Hsie, M. Trainer, R. Tallamraju, and S. C. Liu, A regional model study of the ozone budget in the eastern United States, *J. Geophys. Res.*, 96, 10,809-10,845, 1991.
- National Atmospheric Deposition Program (NADP), World wide web site, <http://nadp.sws.uiuc.edu>, 2002.
- Quinn, P. K., R. J. Charlson, and T.S. Bates, Simultaneous observations of ammonia in the atmosphere and ocean, *Nature*, 335, 336-338, 1988.
- Saxena, P., A. B. Hudischewskyj, C. Seigneur, and J. H. Seinfeld, A comparative study of equilibrium approaches to the chemical characterization of secondary aerosols, *Atmos. Environ.*, 20, 1471-1484, 1986.
- Schere, K.L., Modeling ozone concentrations, *Environ. Sci. Technol.*, 22, 488-495, 1988.
- Seinfeld, J. H. and S. N. Pandis, *Atmospheric Chemistry and Physics*, John Wiley, New York, 1998.
- U.S. Environmental Protection Agency, 1995. *Acid Deposition Standard Feasibility Study Report to Congress*, EPA Report 430-R-95-001a, Office of Air and Radiation, Acid Rain Division, Washington, D.C.
- U.S. Environmental Protection Agency, 1997. *Deposition of Air Pollutants to the Great Waters*, EPA Report 453/R-97-011, Office of Air Quality Planning and Standards, Research Triangle Park, NC.
- Wamsley, J.L. and M.L. Wesley, Modification of coded parameterizations of surface resistances to gaseous dry deposition, *Atmos. Environ.*, 30, 1181-1188, 1996.
- Wesley, M. L., Parameterizations of surface resistances to gaseous dry deposition in regional scale numerical models, *Atmos. Environ.*, 23, 1293-1304, 1989.
- Wesley, M. L., and B. B. Hicks, A review of the current status of knowledge on dry deposition, *Atmos. Environ.*, 34, 2261-2282, 2000.
- Zhang Y., C. Seigneur, J. H. Seinfeld, M. Jacobson, S. L. Clegg, and F. S. Binkowski, A comparative review of inorganic aerosol thermodynamic equilibrium models: similarities, differences, and their likely causes, *Atmos. Environ.*, 34, 117-137, 2000.